Random allocation of blastomere descendants to the trophectoderm and ICM of the bovine blastocyst

L.P. Sepulveda-Rincon, Delphine Dube, Pierre Adenot, Ludivine Laffont, Sylvie Ruffini, Laurence Gall Pouget, B.K. Campbell, Véronique Duranthon, Nathalie N. Beaujean Bobineau, W.E. Maalouf

BIOLOGY OF REPRODUCTION (2016) **95**(6):123, 1–10
Published online before print 19 October 2016.
DOI 10.1095/biolreprod.116.141200

Random Allocation of Blastomere Descendants to the Trophectoderm and ICM of the Bovine Blastocyst[1]

Lessly P. Sepulveda-Rincon,[4,6] Delphine Dube,[4,7] Pierre Adenot,[7] Ludivine Laffont,[7] Sylvie Ruffini,[7] Laurence Gall,[3,7] Bruce K. Campbell,[6] Veronique Duranthon,[7] Nathalie Beaujean,[2,5,7,8] and Walid E. Maalouf[5,6]

[6]*Child Health, Obstetrics and Gynecology, School of Medicine, University of Nottingham, Nottingham, United Kingdom*
[7]*UMR BDR, INRA, ENVA, Université Paris Saclay, Jouy en Josas, France*
[8]*Univ Lyon, Université de Lyon 1, Inserm, Bron, France*

ABSTRACT

The first lineage specification during mammalian embryo development can be visually distinguished at the blastocyst stage. Two cell lineages are observed on the embryonic-abembryonic axis of the blastocyst: the inner cell mass and the trophectoderm. The timing and mechanisms driving this process are still not fully understood. In mouse embryos, cells seem prepatterned to become certain cell lineage because the first cleavage plane has been related with further embryonic-abembryonic axis at the blastocyst stage. Nevertheless, this possibility has been very debatable. Our objective was to determine whether this would be the case in another mammalian species, the bovine. To achieve this, cells of in vitro produced bovine embryos were traced from the 2-cell stage to the blastocyst stage. Blastocysts were then classified according to the allocation of the labeled cells in the embryonic and/or abembryonic part of the blastocyst. Surprisingly, we found that there is a significant percentage of the embryos (~60%) with labeled and nonlabeled cells randomly distributed and intermingled. Using time-lapse microscopy, we have identified the emergence of this random pattern at the third to fourth cell cycle, when cells started to intermingle. Even though no differences were found on morphokinetics among different embryos, these random blastocysts and those with labeled cells separated by the embryonic-abembryonic axis (deviant pattern) are significantly bigger; moreover deviant embryos have a significantly higher number of cells. Interestingly, we observed that daughter cells allocation at the blastocyst stage is not affected by biopsies performed at an earlier stage.

blastocyst, embryo biopsy, H3 arginine methylation, patterning, preimplantation development, time-lapse microscopy

INTRODUCTION

Across evolution, it is usually believed that some earlier developmental mechanisms are conserved because any changes might compromise further developmental events. Nevertheless, early embryonic development is very diverse through all the species [1]. Cell lineage specification mechanisms are well established in nonvertebrate species [2] and in some vertebrates [3], where egg molecules and first cell cleavages have an effect on further development. Therefore, it is believed that cells are prepatterned to be a specific cell lineage since early embryo stages [4]. However, birds and mammals seem to have different developmental routes as this patterning has not been proven [5]. To date, the first crucial factor(s) and the starting point of cell lineage specification are still unknown in mammalian species [6].

The preferred model for mammalian preimplantation development studies so far has been the mouse because this model allows among other factors a wide analysis of its genome and of regulatory networks as well as easy embryo collection and manipulation [3, 7–13]. Latest investigations have been trying to elucidate what is driving cell lineage specification in preimplantation mouse embryos and when the fate of each cell is established. It has been proposed that the first two blastomeres of the mouse embryo present different potential to become part of the embryonic or abembryonic part at the blastocyst stage. While some studies point out that the embryonic-abembryonic axis might be established since syngamy [14–22] under the influence of epigenetic modifications [18, 22], others suggest that cell fate is a random event and is not determined before the 8-cell stage [9, 23–28]. The great plasticity of mammalian embryos against external manipulations—such as rearrangement/removal of blastomeres and in vitro culture—might also interfere with lineage specification patterns [14, 29, 30]. It is therefore still not clear whether there is a hidden pattern in preimplantation mammalian embryos or if cell commitment is just a series of stochastic events. Nevertheless, it has been reported that mouse blastocysts with different patterns are associated with differing developmental potential to form an offspring [18].

The objective of the present study was to observe how the first cleavage is related to cell allocation at the blastocyst stage in the bovine embryo. Additionally, we wanted to investigate the effects of embryo biopsy at the cleavage stage and its

[1]This work was funded by Laboratoire d'Excellence Revive (Investissement d'Avenir, ANR-10-LABX-73). Ph.D. studies of L.P.S.-R. are sponsored by CONACyT Mexico and The University of Nottingham. Ph.D. studies of D.D. are supported by the FRM (FDT20140930876). Presented in part at the 41st Annual Conference of the International Embryo Transfer Society, 10–13 January 2015, Versailles, France.
[2]Correspondence: Nathalie Beaujean, INSERM U1208, INRA USC1361, Stem Cell and Brain Research Institute, 18 avenue Doyen Lépine, 69675 Bron, France. E-mail: nathalie.beaujean@inserm.fr
[3]Deceased.
[4]These authors contributed equally to the work and are considered co-first authors.
[5]These senior authors contributed equally to the work and are considered co-senior authors.

Received: 15 April 2016.
First decision: 12 May 2016.
Accepted: 17 October 2016.

eISSN: 1529-7268 http://www.biolreprod.org
ISSN: 0006-3363

effects on cell allocation patterns at blastocyst stage. Indeed, embryo preimplantation genetic diagnosis/screening is becoming increasingly applied in fertility clinics worldwide with blastomere biopsy on Day 3 remaining the most common technique for obtaining the biological material. To our knowledge, this is the first study in bovine embryos using live cell tracing technology.

MATERIALS AND METHODS

All reagents and chemicals were purchased from Sigma-Aldrich unless otherwise stated.

Ethics

All experiments were performed as stated by the European Convention on Animal Experimentation and the Society for the Study of Biomedical Research Involving Animals. Nathalie Beaujean has authorization to work with laboratory animals from the departmental veterinary regulatory service (license No. 78–95) and from the local ethics committee (No. 12/123, Comethea Jouy-en-Josas/AgroParisTech).

Mouse Embryo Collection

B6CBA F1 females (6–8 wk old) were superovulated with one intraperitoneal injection of 5 IU equine chorionic gonadotropin (Intervet) and after 48 h with an injection of 5 IU human chorionic gonadotropin (hCG) (Intervet). Following the hCG injection, females were placed and mated with B6CBA F1 males (2–10 mo old). Females were sacrificed by cervical dislocation 22–24 h post-hCG. One-cell embryos were collected in prewarmed M2 medium with hyaluronidase (1 mg/ml) and rinsed in M2 medium under mineral oil. Embryos were cultured in M16 medium under mineral oil in a humidified incubator at 37°C with a gaseous atmosphere of 5% CO_2.

Bovine Embryo Production

In vitro maturation and fertilization were carried out as described previously [31]. Briefly, cumulus oocyte complexes (COCs) were aspirated from follicles of 2–8 mm in diameter from bovine ovaries collected from a local slaughterhouse. COCs were rinsed in embryo collection medium (Euroflush; IMV Technologies) and matured in TCM 199 supplemented with 10% fetal calf serum (FCS), 5 μg/ml each of FSH (Folltropin-V; Vetrepharm) and LH (Lutropin-V; Vetrepharm), 1 μg/ml of estradiol, and gentamycin at 50 μg/ml for 22 h at 39°C in 5% CO_2 in air. COCs were repeatedly pipetted until two to five layers of granulosa cells were left around the oocyte. Groups of 50 COCs were then incubated in 0.5 ml of frozen/thawed sperm at a concentration of 1.0 mole/ml of fertilization medium and cultured for 18 h at 39°C in a humidified incubator with an atmosphere of 5% CO_2 in 95% N_2. Fertilized embryos were rinsed and cultured in SOF medium (Minitube) with 1% estrus cow serum and amino acids at 39°C in 5% CO_2, 5% O_2, and 90% N_2. The next day (Day 1), all embryos were washed twice in HEPES buffer modified with synthetic oviductal fluid (H-SOF) medium and transferred into mSOFaa media supplemented with 3 mg/ml of bovine serum albumin (BSA) for 24 h. On Day 2, cleaved embryos were transferred into fresh mSOFaa media supplemented with 10% FCS. Embryo culture was carried out at 39°C in a humidified incubator with a gaseous atmosphere of 5% CO_2, 5% O_2, and 90% N_2.

Labeling of Blastomeres at the 2-Cell Stage

The long-chain dialkylcarbocyanines lipophilic tracer 1,1′-dioctadecyl-3,3,3′,3′-tetramethylindocarbocyanine perchlorate (DiI) (D3911, lot no. 1072939; Molecular Probes) was dissolved in virgin olive oil at 60°C at a final concentration of 2 mg/ml. When cooled down and prior to labeling, the microinjection pipette was backfilled with the dye. The injections were performed on a Nikon Diaphot-TMD inverted microscope using Narishige micromanipulators with a coupled Eppendorf 5242 microinjector. For micromanipulation, mouse embryos were placed in M2 media and bovine embryos were placed in embryo-holding medium (IMV Technologies) containing 10% FCS. Injection of one blastomere with the tracer DiI was performed at the 2-cell stage (46–48 h post-hCG in mouse and ~30–32 h postfertilization in bovine). The micropipette was pushed through the zona pellucida and pressed against one of the blastomere membrane and a microdrop of DiI was then deposited as previously described [19].

For double blastomere labeling, injection of one blastomere with DiI was performed first in all embryos. The injection pipette was then changed, and the second injection was performed with the same equipment as above. The oil drop from the DiI injection allowed us to identify the first injected blastomeres, and the twin blastomere was then injected in the cytoplasm with a solution of 150nM Ras-eGFP mRNA (kind gift from Nadine Peyriéras and Dimitri Fabrèges, Institut de Neurobiologie Alfred Fessard), which labels the cytoplasmic membrane [32].

Time-Lapse Recording of Bovine Embryo Development

Time-lapse observations in bovine were performed on a Zeiss LSM700 confocal microscope (MIMA2 platform; INRA). The inverted microscope AxioObserver Z1 is coupled with an incubation system including a heating insert P stage, a XL incubator chamber, and an incubator S for delivering of CO_2. All insert and incubators are regulated by specific controllers (TempModule S, Heating Unit XL S, and CO_2 Module S) purchased from Carl Zeiss, Inc. For time-lapse observations, embryos (maximum of six) were cultured in 20 μl drop of SOF medium in IBIDI dish with glass bottom and placed on the inverted microscope with the incubator chamber at 38.5°C and 5% CO_2. Bright field and fluorescence images within different focal planes with 7 μm intervals were recorded, with Zeiss Zen software, every 2 h using a Plan-Apochromat 20× NA 0.8. To improve the signal detection and to decrease toxicity by irradiation, we used a 2.5 Airy unit pinhole size (scaling Z = 7.2 μm) and laser power equal to 0.2% of maximum (laser at 488 nm of 10mW, laser at 555 nm of 1mW). Embryos were followed until the 8- to 16-cell stage and then either returned to culture in the same IBIDI dish up to the blastocyst stage or left under the microscope up to the blastocyst stage with 6 h intervals between each acquisition.

Cleavage Stage Embryo Biopsy

For embryo biopsy at the cleavage stage, bovine embryos were assessed at 44–46 h post-IVF and 8- to 12-cell embryos were randomized for biopsy. Briefly, embryo biopsy was performed using a 40× XY Clone laser objective (Hamilton Thorne Biosciences) mounted on a Leica DMI3000 B inverted microscope. The holding pipette used had a length of 60 mm, an internal diameter of 9–17 μm, and a bevel of 30° (Swemed; Vitrolife). The biopsy pipette used had a length of 1900 μm, an internal diameter of 19 μm, and a bevel of 35° (Eppendorf) for mouse embryos and an inner diameter of 30 μm and a bevel of 35° (G32795; Cook Medical) for bovine embryos. During biopsy procedure embryos were handled in 5-μl drops of G-PGD medium (Vitrolife) under mineral oil. Zona opening was performed with a 300 μsec pulse noncontact laser at 100% power. Then, a single blastomere was randomly removed and the resulting biopsied embryos were further cultured until the blastocyst stage under culture conditions.

Cell Allocation Assessment at the Blastocyst Stage

Fluorescence microscopy for observation of DiI staining in mouse and bovine blastocysts was performed either on a Nikon Diaphot-TMD inverted microscope equipped with a 40× fluorescence objective, an ultraviolet filter cube, and a Nikon D7000 camera connected to the microscope or under an inverted microscope AxioObserver Z1 equipped with a Colibri LED illumination system and an Axiocam MRm camera. Images were acquired with red and green fluorescent filters that correspond to the excitation/emission wavelengths of DiI (EXmax = 553 nm, EMmax = 570 nm) and eGFP (EXmax = 488 nm; EMmax = 509 nm). During observation, mouse blastocysts were placed in M2 media at 37°C and at 39°C for bovine embryos. Blastocysts were rotated placing the blastocoel cavity floor and the boundary line between the fluorescent and nonfluorescent cells in the same focal plane, as previously described [33].

Blastocysts were classified into three categories: orthogonal, deviant, and random. The orthogonal pattern was attributed to blastocysts that demonstrate an angular degree between the boundary line of the fluorescent and nonfluorescent cells and the blastocoel cavity floor $\leq 30°$ with two well-defined cell clusters (fluorescent and nonfluorescent), in other words, if labeled cells were allocated either in the embryonic or abembryonic part of the blastocyst. The deviant pattern was attributed to blastocysts that demonstrated an angular degree of $>30°$. The pattern called random was attributed to blastocysts that presented labeled cells within the whole embryo with different clusters of labeled cells.

Histone H3 Methylation at Arginine 2 Immunolabeling and Quantification

Embryos at the 4-cell stage were fixed overnight at 4°C with 4% (w/v) paraformaldehyde diluted in PBS and then permeabilized with 0.5% (v/v)

Triton X-100/PBS (30 min, at room temperature). Embryos were then incubated with 2% BSA-PBS for 1 h. Incubation with the rabbit polyclonal anti-H3R2me2 (histone H3 methylation at arginine 2) antibody (05-808, dilution 1:200; Merck Millipore) was performed overnight at 4°C. After two washes with PBS, embryos were incubated 1 h at room temperature with an Alexa Fluor 488-conjugated secondary antibody (dilution 1:500; Life Technologies). Both antibodies were diluted in 2% BSA-PBS. After two supplementary washes with PBS, DNA counterstaining was performed with TO-PRO-3 Iodide (1 μM in PBS; Thermo Fisher Scientific) for 15 min at room temperature. Embryos were then mounted on slides with an antifading agent (ProLong antifade mountant; Molecular Probes). Observation were performed with a Leica SPE confocal laser scanning microscope equipped with an oil immersion objective (Plan Apochromatic 40× NA 1.25), with the 488- and 635-wavelengths lasers. Entire embryos were scanned with a distance between light optical sections of 0.37 μm. For signal quantification, maximum intensity projections of Z-stacks were performed using ImageJ software and the nuclei were outlined manually. Total fluorescence intensities were calculated from these projections by multiplying the mean fluorescence intensities and nuclear areas. Fluorescence levels were then normalized against the blastomere showing the highest level, which was set at 100%.

Sox2 Immunolabeling and Cell Counting

After pattern attribution, the bovine blastocysts at Day 7 were fixed in 4% paraformaldehyde overnight at 4°C. Embryos were rinsed in PBS for 10 min and then permeabilized with 1.0% Triton X-100/PBS for 1 h at room temperature. Furthermore, embryos were placed in boiling 10 mM sodium citrate buffer and maintained at a subboiling temperature for 10 min for the antigen unmasking procedure. The samples were rinsed in PBS and then incubated with 2% (w/v) BSA-PBS for 1 h. Then the embryos were incubated in mouse monoclonal anti-Sox2 antibody (1:50 in 2% BSA-PBS; R&D Systems) for 4 h at room temperature. Embryos were rinsed in PBS solution and then were incubated with an anti-mouse secondary antibody (1:500 diluted in PBS-BSA; Jackson Immunoresearch) for 45 min at room temperature. The embryos were rinsed in PBS and the nuclei were stained with 4′,6-diamidino-2-phenylindole (DAPI) and mounted on the glass slide with antifading medium (Citifluor; Biovalley). The immunofluorescent-labeled embryos were observed under an inverted fluorescent microscope (Axioplan imaging Apotome apparatus; Zeiss) (MIMA2 Platform; INRA). The total number of the DAPI-positive cells and inner cell mass (ICM) cells with Sox2 signal were counted using the cell counter plugin of ImageJ software.

Statistical Analysis

The dataset for total cell counts (TCC) and ICM/total cell ratio were checked for normality using Kolmogorov-Smirnov/Shapiro-Wilk test (IBM SPSS version 22). Analysis of variance ANOVA test was performed to determine any difference between mouse and bovine H3R2me2 staining, incidence of blastocysts patterns, TCC and ICM/total cell within the classified blastocysts, and the Bonferroni post hoc test was performed to determine any difference between random, orthogonal, and deviant groups.

RESULTS

DiI Allocation in Blastocysts

Cell tracing experiments started by labeling one blastomere from the 2-cell bovine embryo followed by observation of daughter cells allocations at the blastocyst stage. This procedure was replicated 40 times. The safety of the injection was assessed by the survival rate after the injection of the lipophilic tracer DiI in bovine 2-cell stage embryos that reached 88.4% ± 1.4% (SEM) followed by a blastocyst rate of 44.4% ± 2.1% compared to 34% ± 1.7% for noninjected control embryos ($P = 0.19$ chi square test). On Day 7, the embryos that reached the blastocyst stage were analyzed under a fluorescence microscope to determine the distribution of the labeled and unlabeled cells. We observed the two expected types of blastocysts with two defined clusters of cells (fluorescent and nonfluorescent): 1) the orthogonal blastocysts with an angular degree between the boundary line of the labeled and unlabeled cells and the blastocoel cavity floor $\leq 30°$ and 2) the deviant blastocysts demonstrating an angular degree of $>30°$, as previously described [27]. Surprisingly, a third cell allocation pattern was found in the bovine blastocysts (Fig. 1A). In this latest case, blastocysts presented several clusters of labeled cells and unlabeled cells dispersed within the whole embryo (Fig. 1A); we termed this pattern random.

Unfortunately, we had some blastocysts with no labeling due to the arrest of the injected blastomere or fading of the staining. We also encountered some collapsing of a number of blastocysts during classification. Despite this, a total of 346 bovine blastocysts were classified with 62.9% ± 2.6% as random, 14.9% ± 2.3% as orthogonal, and 22.2% ± 2.6% as deviant (Fig. 1B). Highly significant differences were found in the incidence of the random pattern as opposed to the orthogonal and deviant ones ($P < 0.001$), underlying the fact that this random pattern is the most frequent one observed in this species. We reproduced the same experiments type of labeling and cell tracing experiment in mouse to know if we could also observe this random pattern in mouse blastocysts. Of 12 repetitions of the experiment, a total of 459 blastocysts (77.4% ± 4.0% blastocyst rate after DiI injection) could be classified according to their cell allocation patterns. As in bovine embryos, we report a similar distribution of the three patterns in mouse embryos, although we observed a lower proportion of random mouse blastocysts (46.1% ± 0.05% vs. 22.7% ± 0.03% for orthogonal and 31.25% ± 0.03% for deviant embryos) (Fig. 1B and Supplemental Movie S1; Supplemental data are available online at www.biolreport.org). The difference was highly significant between the orthogonal and random cell lineage allocation patterns ($P = 0.001$) and less significant between deviant and random patterns ($P = 0.053$).

Blastomeres Tracing in Bovine Embryos by Time-Lapse Microscopy

To explain the occurrence of the random pattern in bovine embryos, we hypothesized that daughter embryonic cells got intermingled at some point during the preimplantation development. In order to have a better visualization of this process, new batches of labeled embryos were monitored by time-lapse microscopy. We used two different types of labeling procedure. Either only one blastomere was labeled with the lipophilic tracer DiI at the 2-cell stage as above. Alternatively, each blastomere of two-cell embryos was injected with a different dye from its counterpart, either with lipophilic tracer DiI or with Ras-eGFP. Because these two tracers have different excitation/emission wavelengths, we could clearly follow all the daughter cells from each blastomere.

Following labeling at the 2-cell stage (on Day 2 postfertilization) and overnight culture, embryos were transferred in the glass bottom dishes for 24 h time-lapse observations (between 44 and 72 h postinsemination) and returned to normal culture conditions after this period. When the observations started on Day 3, most embryos had already cleaved and presented either three to four cells (n = 18, 50%) or five to seven cells (n = 15, 41.7% out of 36 embryos from seven replicates; Supplemental Table S1). A small proportion of the embryos were still at the 2-cell stage (n = 3, 8.3%).

On Day 4, at the end of the time-lapse observation, only three embryos did not develop further and were blocked. In all the other embryos, at least one blastomere cleaved and even reached the next cell cycle (Supplemental Table S1): those with three to four cells reached five to eight cells (n = 13, 76.5% at the fourth cell cycle) or even more (n = 4 with nine to 13 cells, 23.5% at the fifth cell cycle), and most of those at five to seven cells reached the fifth cell cycle (n = 9, 60% with nine to 14 cells). When we looked at the labeling, we distinguished two types of embryos (Fig. 2, Supplemental Table S1): those with

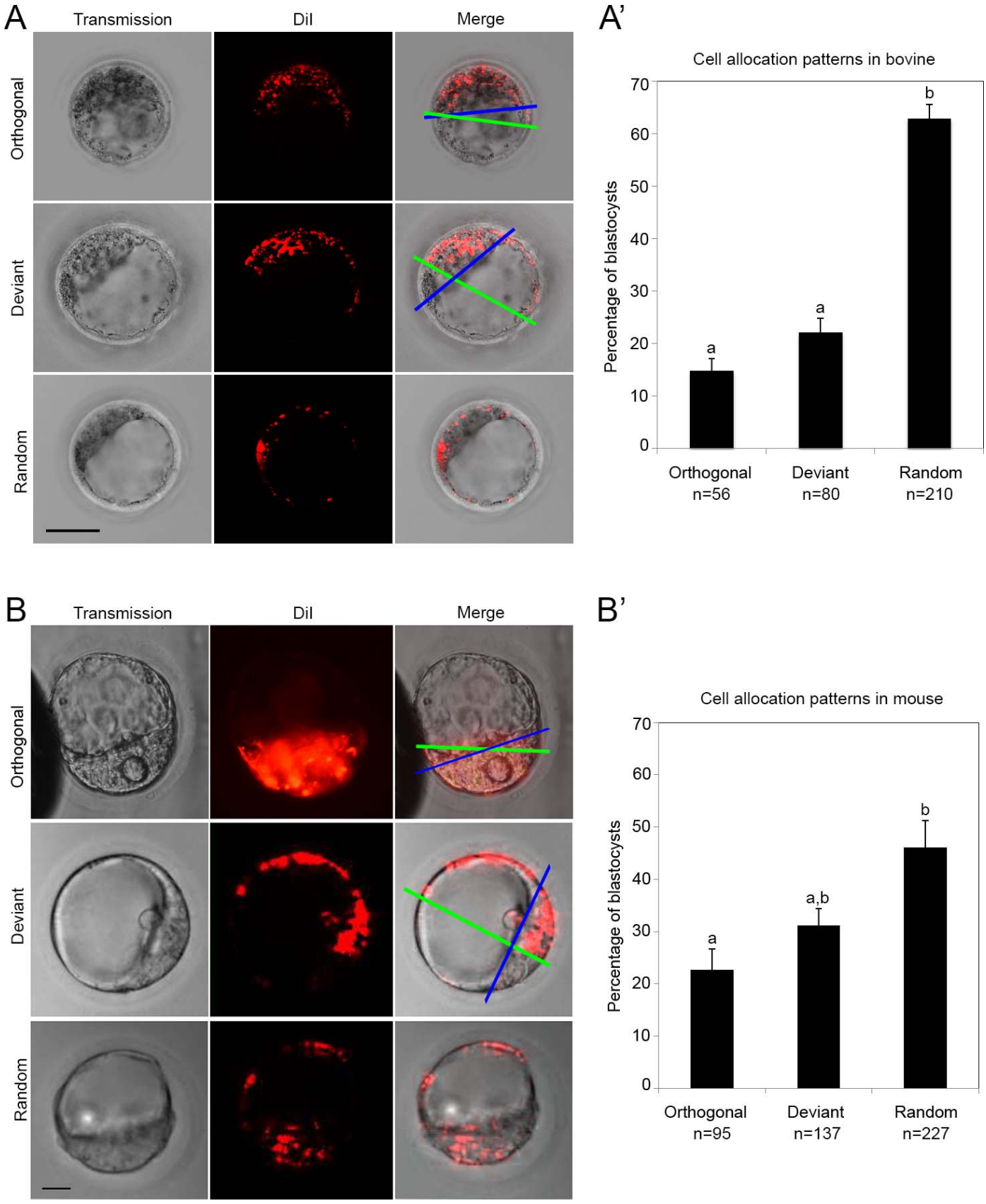

FIG. 1. Cell-allocation patterns at the blastocyst stage. Examples of bovine (**A**) and mouse (**B**) blastocysts observed after DiI labeling (Z-projections of the Apotome images) with drawings of the boundary line between the labeled/unlabeled cells (green) and the blastocoel cavity floor (blue). According to the angle between these two lines ($\leq 30°$ or $>30°$), blastocysts were scored as orthogonal or deviant, respectively. When the labeled and nonlabeled cells were intermingled, making it impossible to draw a boundary line between them, blastocysts were scored as random. Bar = 50 μm for bovine embryos and 20 μm for mouse embryos. The proportion of the different cell allocation patterns observed at the blastocyst stage after DiI labeling, in bovine (**A'**) and

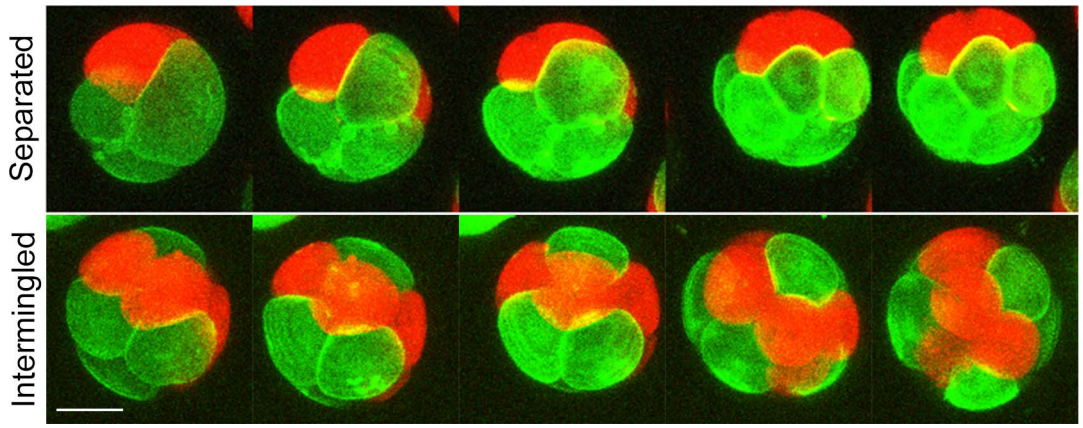

FIG. 2. Sequential images of Day 3/Day 4 bovine embryos labeled with DiI and Ras-GFP. Examples of the separated and the intermingled pattern observed in bovine embryos labeled at the 2-cell stage with the lipophilic tracer DiI in one blastomere and with Ras-eGFP in the other one. The selected images correspond to three-dimensional reconstructions obtained with the Zeiss Zen software from the time-lapse movies (Supplemental Movies S1 and S2), with a 4-h interval. Bars = 50 μm.

daughter cells of each blastomere clearly grouped into two separated clusters (labeled and nonlabeled) (n = 17, 47.2%; Fig. 2 upper panel) and those showing an intermingled pattern with some daughter cells of one blastomere inserted among the daughter cells of the other blastomere (n = 13, 36.1%; Fig. 2 lower panel). This intermingled pattern was already observed in 37.5% of the embryos with seven to eight cells (n = 6 out of 16) and in 53.8% of the embryos with nine to 13 cells (n = 7 out of 13), suggesting that the intermingling event may occur during the transition from the fourth to the fifth cell cycle. Surprisingly, this pattern was the most frequent one observed in embryos that were already at seven cells on Day 3 (n = 3 out of 4, 75%) and in embryos that already reached 11 to 14 cells on Day 4 (n = 5 out of 6, 83%). In contrast, embryos which developed into blastocyst with four to six cells on Day 3 and eight to 10 cells on Day 4 exhibited mostly a pattern with clear separation between daughter cells (n = 8 out of 12; 67%). This suggests that the intermingled pattern could result from an abnormally fast development during the first cell cycles. However, when we analyzed the speed of cell cleavage of each 2-cell blastomere and its daughter cells, no correlation could be found to explain the appearance of the characteristic intermingled pattern. We also did not observe difference in terms of cell death or arrest between the daughter cells of the injected versus noninjected blastomeres.

After 24-h time-lapse observations, the embryos were returned into culture. Those embryos were able to develop to the blastocyst stage (n = 23, 63.8% on Day 7). We did not observe a strong difference between the two labeling procedures (seven of 14 blastocysts with single DiI labeling and 16 of 22 with double DiI/Ras-eGFP labeling, $P = 0.3$ chi square test). Among those blastocysts, the random pattern was detected in 13 embryos (56.5%), and the deviant or orthogonal patterns were only found in 10 embryos (43.4%), underlying again the predominance of the random pattern in bovine blastocysts. Interestingly, we observed that experimental replicates with a high frequency of intermingled pattern at Day 4 (>60%) had a higher rate of random blastocysts (>75%, in three experiments out of six) and that replicates with a higher frequency of separated pattern (>75%) gave a higher rate of deviant and orthogonal blastocysts (>67%, two experiments).

Further, we observed 12 embryos on time-lapse up to the blastocyst stage. Under these conditions, 50% were able to develop to the blastocyst stage (n = 6 out of 12). Remarkably, we observed that the only random blastocyst we got on Day 7 was classified as intermingled on Day 4 (Fig. 3, A and A'). All the others—classified as separated on Day 4—became deviant blastocysts on Day 7 (Fig. 3, B and B').

Blastocysts Quality

When we analyzed DiI allocation in embryos on Day 7 after culture in the usual culture conditions (90% O_2, 5% CO_2, and 5% O_2 mixture in the incubator at 39°C), we also evaluated their stage of development according to International Embryo Transfer Society manual's standards [34]. We classified the blastocysts in two groups: stage 6 blastocyst and stage 7–8 expanded or hatched blastocyst (Fig. 4). We combined both parameters and found that the majority of orthogonal embryos were stage 6 blastocysts whereas deviant and random ones were mostly stage 7–8 blastocysts ($P < 0.001$). We tried to correlate those differences with the total number of cells. Then we analyzed the total cell number by DNA staining and significant difference was observed between the deviant embryos presenting 140.2 ± 8.6 cells (n = 23 embryos) compared with orthogonal embryos presenting 91.2 ± 11.1 cells (n = 15, $P < 0.001$) and random embryos presenting 108.4 ± 4.7 cells (n = 45, $P = 0.004$). There was no difference between orthogonal and random groups ($P = 0.365$).

We also analyzed the ICM/total cell ratio by SOX2 immunolabeling, a protein found specifically in the ICM cells (Fig. 5) [35]. No significant difference was found among the patterns concerning the ICM/total cell ratio ($P = 0.144$). Where the orthogonal embryos presented an ICM/total cell ratio of 0.34 ± 0.06 (n = 7), deviant embryos presented a ratio of 0.35 ± 0.03 (n = 15) and random embryos presented a ratio of 0.28 ± 0.02 (n = 26).

mouse (**B'**). Expressed values represent the mean percent ± SEM of each pattern among repetitions of the experiment. The total number of blastocysts scored is indicated below each column. For each graph, values with different superscripts (a, b) indicate significantly different values ($P < 0.05$; Bonferroni post hoc test).

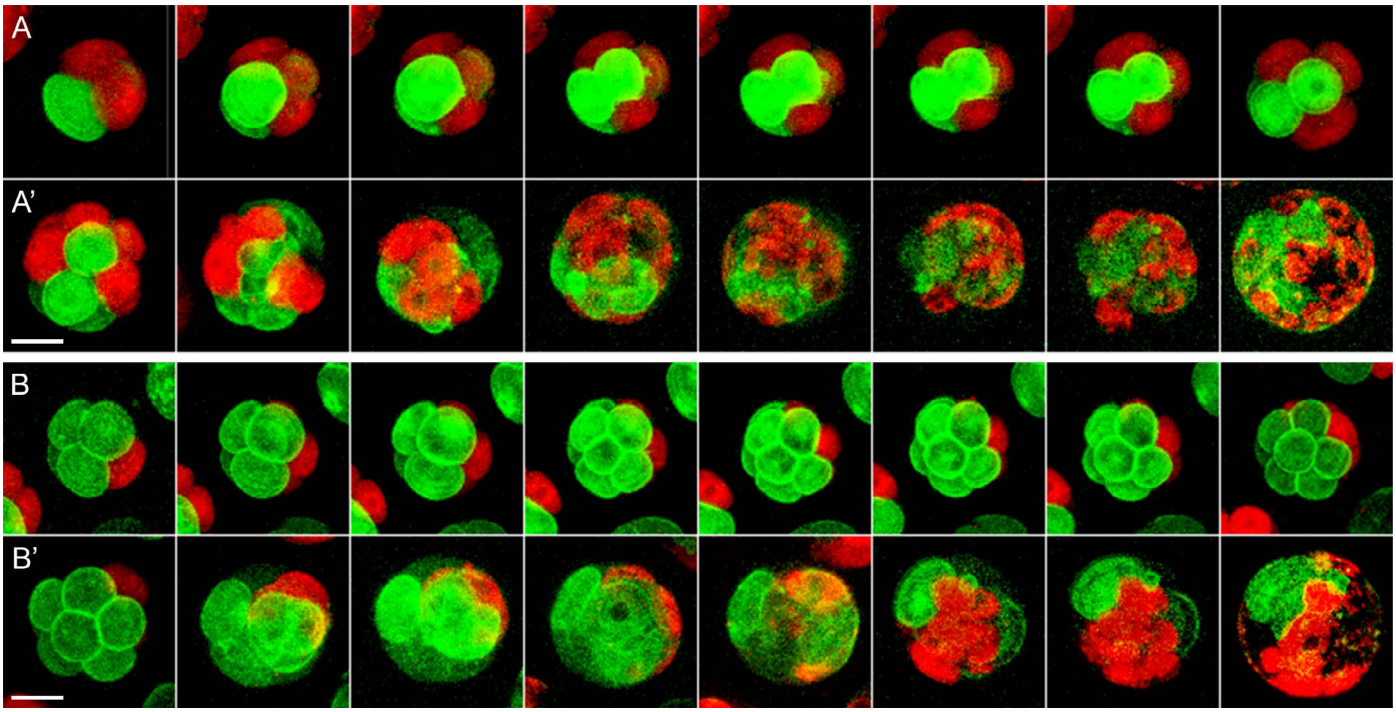

FIG. 3. Sequential images of labeled bovine embryos up to the blastocyst stage. Bovine embryos with the DiI/Ras-GFP double labeling were observed by time-lapse microscopy from Day 3 up to the blastocyst stage. Examples (three-dimensional reconstructions) shown here correspond to images taken every 4 h between Day 3 and 4 (**A**, **B**) and then every 12 h (**A′**, **B′**). Whereas the bovine embryo with an intermingled pattern (**A**) became a random blastocyst (**A′**), the separated one (**B**) became a deviant blastocyst (**B′**). Bars = 50 μm.

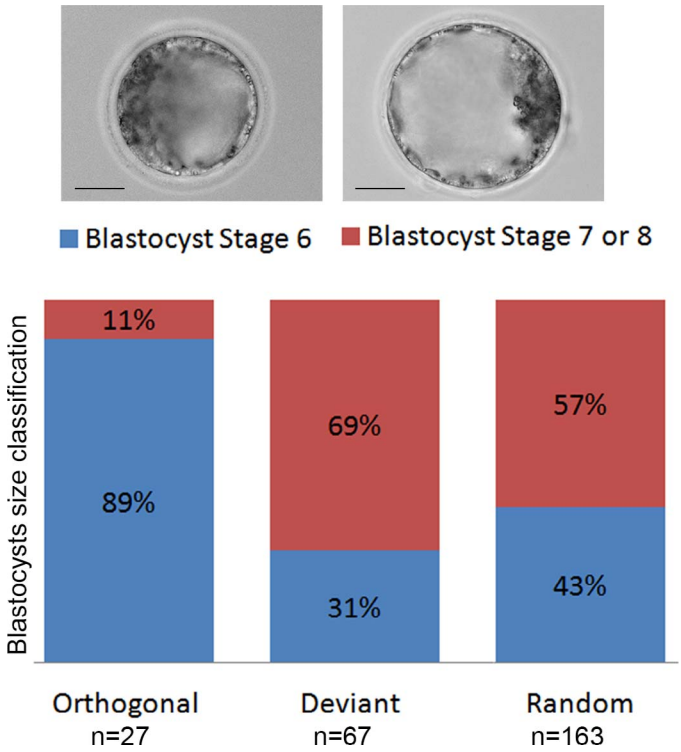

FIG. 4. Scoring of the bovine blastocyst according to their size. Bovine blastocysts were classified into two groups: stage 6 blastocyst and stage 7–8 expanded/hatched blastocyst and were then analyzed for their DiI allocation. Examples of each type of blastocyst (bars = 50 μm) are shown on top of the graph that combines both parameters. The total number of blastocysts scored is indicated below each column.

DiI Allocation in Blastocysts after Single Blastomere Removal

After DiI injection at the 2-cell stage, a total of 156 bovine embryos at 8- to 12-cell stage were biopsied in five repetitions of the experiment. From those, 107 embryos reached the blastocyst stage (68% ± 9.9%). The bovine blastocysts showed the three cell-allocation patterns previously described with the following incidence: orthogonal pattern 21% ± 3.4%, deviant pattern 16% ± 4.2%, and random pattern 63% ± 1.4%. The incidence of the different cell-allocation patterns of the biopsied embryos is not significantly different from the nonbiopsied embryos ($P > 0.05$). Yet, the difference on the incidence between patterns is significant ($P < 0.001$). Post hoc Bonferroni test showed that this difference can be attributed mainly to the difference between the incidence of the random pattern compared with the orthogonal ($P < 0.001$) and the deviant one ($P < 0.001$). This tendency is the same as the one observed in the control group.

Overall, univariate test showed no significant difference ($P = 0.080$) between the TCC of biopsied and nonbiopsied embryos. However, a further *t*-test suggested a tendency of TCC decrease of the biopsied embryos toward deviant (95.8 ± 15 cells, n = 12, $P = 0.018$) and random embryos (90.6 ± 6.6 cells, n = 31, $P = 0.004$) when compared with their nonbiopsied counterparts. Yet, orthogonal embryos were not affected by the biopsy procedure ($P = 0.065$). Biopsied orthogonal embryos presented a TCC of 116.6 ± 10.6, similar to their nonbiopsied counterparts (n = 18, $P > 0.05$).

H3R2me2 in 4-Cell Bovine Embryos

Because histone H3 arginine methylation (H3R26me and H3R2me2) seems to regulate the contribution of the 4-cell stage blastomeres to the ICM in the early mouse embryo [18,

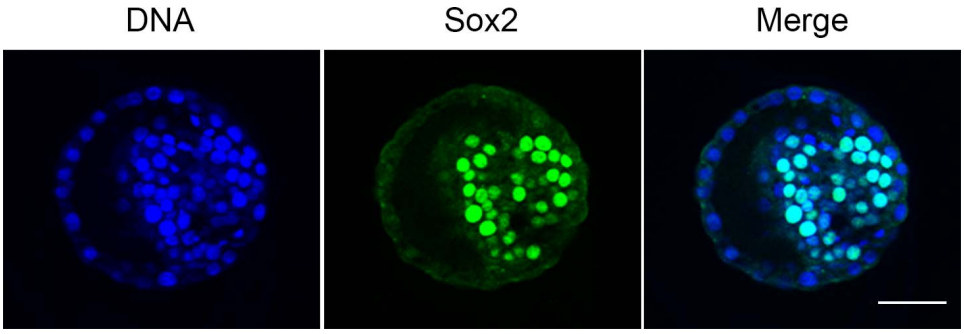

FIG. 5. Immunodetection of SOX2. Immunodetection of Sox2 (green) and labeling of DNA by DAPI (blue) was performed in each group of bovine blastocysts (bar = 50 μm). The total number of DAPI- and SOX2-positive cells was determined on z-projections using the cell counter plugin of ImageJ software.

22], we hypothesized that H3R2me2 levels at the 4-cell stage could be different in bovine embryos. We therefore performed immunodetection of this posttranslational histone modification on bovine 4-cell embryos. Quantification of the staining shows that bovine 4-cell embryos present a significant difference in H3R2me2 levels between their blastomeres ($P = 0.03$, n = 35; Fig. 6). However, these differences between blastomeres are not lower or greater than in mouse (n = 15, Fig. 6) suggesting that blastomeres in bovine embryos have a similar epigenetic potential as mouse embryos.

DISCUSSION

Cell Tracing and Allocation Assessment

In the present study, we have applied for the first time an effective cell tracing method in preimplantation bovine embryos. As previously reported [18], our results showed that the use of lipophilic tracers on mammalian embryos is not detrimental for their development. Bovine blastocyst rates were indeed quite similar in the injected group (44.4%) in comparison to the noninjected embryos that were kept in culture (34%). Regarding the damage induced by microinjection, we obtained a higher proportion of blastocysts in bovine with developmental arrest of the injected blastomere than in mouse; however, the rate was under 15% for both species (data not shown). Even without micromanipulation, this phenomena has been observed frequently in bovine embryos across the literature both in vivo and in vitro [36].

The literature reports controversial results in mouse embryos regarding the predisposition of the two-cell embryo blastomeres to become a specific cell lineage. Our results can only be compared with those reported in mouse embryos because other mammalian species have not been studied with the exception of partenogenetically activated pig embryos [37, 38] and ovine embryos [39]. Our results differ from those reported in mouse, where in the majority of the embryos (>60%) the first cleavage plane will be orthogonal to the embryonic-abembryonic axis (orthogonal group) [17, 19, 20,

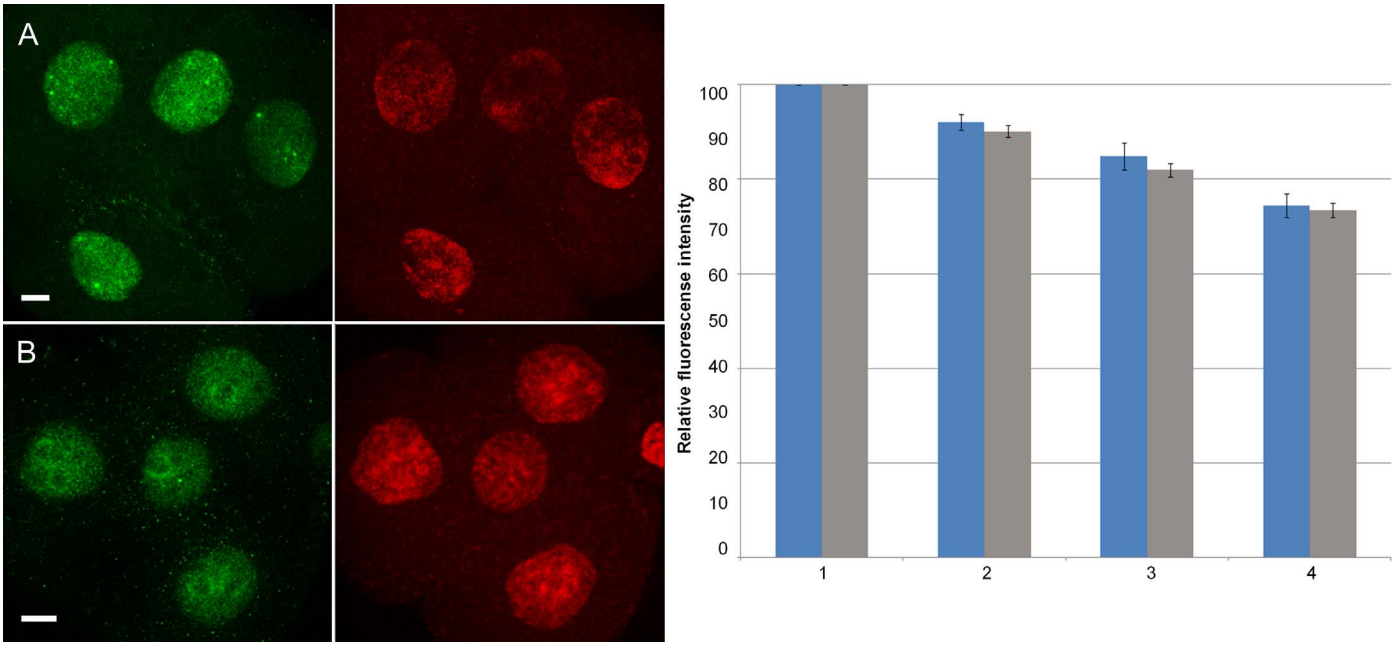

FIG. 6. Immunodetection of histone H3 arginine methylation. Immunodetection of H3R2me2 (green) and labeling of DNA (red) was performed in bovine (**A**) and mouse (**B**) 4-cell stage embryos (bar = 10 μm). Quantification was then performed with ImageJ software as described in *Materials and Methods*. Each bar represents the relative H3R2me2 fluorescence level of one of the four blastomeres either in bovine (blue bars, n = 35) or mouse (gray bars, n = 15) embryos. The results for the two species are not statistically different ($P > 0.05$), however there is significant differences between blastomeres ($P = 0.03$).

40]. In our study, only ~15% of the embryos were orthogonal in both species. These results resemble those reported in parthenogenetic activated porcine embryos where random pattern is more predominant [38]. A similar tendency was shown in ovine embryos [39]. These comparisons might have limitations due to the different oocyte maturation and fertilization protocols. Indeed, our experiments in bovine have been performed on in vitro matured and fertilized embryos, whereas mouse embryos are produced in vivo. On the other hand, other authors have suggested that the high proportion of orthogonal embryos is due to the restriction of cell movement that affect the zona pellucida shape [23, 28]. It would be worth investigating this question with bovine embryos because their zona pellucida composition is quite different with five glycoproteins versus only three in the mouse [41].

Surprisingly, in the mouse studies, the authors have only reported the incidence of prepatterned embryos, orthogonal and deviant, but a random distribution of the blastocyst cells has not been described in those publications. Cell intermingling has been previously observed [15], but the authors explained that most of the cell mixing occurs after the blastocyst stage. The higher number of cells in bovine Day 7 blastocysts than in mouse blastocysts may explain why it was easier to observe this phenomenon in bovine. In one of the first studies in mouse, blastocysts were classified according to the number of cells that have crossed the boundary line between labeled and unlabeled cells [19]. Those embryos with cells that crossed the boundary line may well correspond to our random embryos. We noticed that the deviant and the random pattern were indeed sometimes difficult to distinguish, especially in the small mouse blastocysts, and that rotation of the blastocyst to clearly locate labeled and unlabeled cells was essential.

Predominance of the Random Distribution at the Blastocyst Stage

Even though the prepatterning theory is still debatable in mammalian embryos, in the present study, we clearly observed both prepatterned (orthogonal and deviant embryos) and nonprepatterned (random embryos) embryos in mouse and bovine species. Literature reporting the incidence of prepatterned and stochastic embryos is scarce and contradictory. While some studies in mouse reported that the deviant pattern is seen in the minority of the embryos [14, 15], other evidence points out to the absence of predetermination [24]. Our results highlight that nonprepatterned (random embryos) represents the majority in bovine (~60%) as has been reported also in ovine embryos [39]. It is worth noticing that nonpatterned embryos are also quite frequent in mouse embryos (~50%). Overall, our results suggest similarities between species in the occurrence of the three blastocyst classifications, suggesting some behavioral resemblance regarding cell fate between mammalian embryos.

In mouse, it has been reported that the methylation of histone H3 arginine targeted by CARM1 may regulate pluripotency and cell fate decision toward the ICM at the blastocyst stage [22]. Indeed, it seems that molecular heterogeneity in OCT4, CARM1, and SOX2 between blastomeres at the 4-cell stage is leading to a biased lineage segregation [42, 43]. We found that H3 arginine methylation differences between blastomeres at the 4-cell stages in bovine embryos do not differ from the ones observed in mouse embryos. However, in bovine, OCT4 and SOX2 cannot be detected at that stage and only accumulate in embryonic nuclei later on [35]. This could explain, at least partially, the lower incidence of the bias toward the ICM in this species as compared to mouse.

Visible daughter cell separation was observed in bovine embryos starting from the 7- and 8-cell stage. Our results differ from those suggesting that cell intermingling in mouse embryos occurs upon blastocoel formation [24] but are in agreement with the intense cell movement observed from the fourth cell cycle onward in both mouse and bovine embryos [44, 45]. Interestingly, our results suggest that random blastocysts most probably emanate from the intermingled Day 4 embryos whereas the other ones (deviant and orthogonal) emanate from Day 4 embryos with separated labeled and nonlabeled cells. We can therefore hypothesize that the process involved in cell intermingling during early preimplantation development may indeed affect cell allocation at the blastocyst stage. The cause of these increased cell movements during preimplantation development is still unknown.

Cell Allocation Patterns Might Be Related to Blastocyst Size

First, we observed that the orthogonal group presented a smaller blastocyst size in bovine embryos. This might be a sign of delayed embryonic development or it might be related to embryo gender, as previously reported [46]. It is also well established that male and female bovine embryos are different in terms of transcriptomic, epigenetic, and protein intake levels [47, 48]. We performed embryo sexing and observed that random and deviant blastocysts had an equilibrated sex ratio, while orthogonal embryos seemed to be female biased (data not shown). These results would fit with the idea that male blastocysts form first, displaying higher TCC [46]. However, getting enough blastocysts to have statistically significant results and determine if cell allocation pattern is related to embryo gender was unachievable.

On the other hand, the ICM/total cell ratio was similar to previously data reported for bovine fertilized embryos, that is, around 0.2–0.4 [49], and was not significantly different between the three blastocyst classifications. There is a tendency for the random group to have lower ICM/total cell ratio value, while orthogonal and deviant embryos have a tendency to present higher ICM/total cell ratios. Further investigations are needed in order to determine if these cell allocation patterns are related to embryo quality and further embryo development. Indeed, a high proportion of ICM cells has been reported to be a principal cause of implantation failure in bovine somatic nuclear transfer blastocysts [50].

Single Blastomere Removal at Cleavage Stage Does Not Affect Cell Allocation Patterns

To our knowledge, this is the first study analyzing the effects of cell removal during the cleavage stage of embryo development on cell allocation carried out by performing a biopsy on a single blastomere around the 8-cell stage in bovine embryos. We report for the first time that embryo biopsy at this stage does not seem to alter the cell-allocation patterns, suggesting that this cell behavior is established earlier in development than the 8-cell stage in bovine embryos. The clinical advantage of using a bovine model is its similarities with human embryos in terms of timing of key embryonic events such as embryonic genome activation at the 8- to 16-cell stage [31], compaction after the 16-cell stage [8], and similar transcriptomic profile [51]. Our results are in agreement with those reported on the literature where TCC is not affected by the biopsy procedure [52, 53]. However, additional analysis

within each cell-allocation pattern group showed that TCC of blastocysts within the deviant and random groups, but not the orthogonal group, were significantly affected by the biopsy procedure. It might be that different types of embryos are affected differently by embryo biopsy and the way embryo cells arrange during preimplantation trigger different compensatory mechanisms.

In conclusion, our findings suggest that cell allocation patterns seem to be related with the total cell number at the blastocyst stage in bovine embryos but not with the ICM/trophectoderm ratio. On the other hand, blastomere removal at the 8-cell stage does not have further implications on cell-allocation patterns at the blastocyst stage, suggesting that cell-allocation patterns are established before the 8-cell stage. Take home baby rates after clinical assisted reproductive technologies are still low; therefore, it is necessary to differentiate between embryos with higher chances of becoming a healthy offspring (that apparently they look the same) before embryo transfer. Studying cell-allocation patterns during preimplantation development might shed some light on this matter. Further research is needed in order to determine if embryo cell-allocation patterns are related to different coping mechanisms after embryo manipulations, implantation, and/or further embryo development.

ACKNOWLEDGMENT

We dedicate this paper in memory of Dr. Laurence Gall, who was instrumental in developing research on bovine embryos in our laboratory from 2008 to 2014. We thank Nadine Peyriéras and Dimitri Fabrèges for RAS EGFP mRNA. We also acknowledge the platform MIMA2 (Microscopie et Imagerie des Microorganismes, Animaux et Aliments) for microscopy equipment, Mr. V. Brochard for the assistance on microscope setup and UE IERP (Unité Expérimentale d'Infectiologie Expérimentale des Rongeurs et Poissons) for animal care.

REFERENCES

1. Slack JMK. Evolution and development. In: Essential Developmental Biology, 3rd ed. Cambridge: John Wiley & Sons, Ltd.; 2013:419–439.
2. Wolpert L, Tickle C, Lawrence P, Meyerowitz E, Robertson E, Smith J, Jessell T. Morphogenesis: change in form in the early embryo. In: Wolpert L, Tickle C (eds.), Principles of Development, 4th ed. Oxford: Oxford University Press; 2011:289–328.
3. Hiiragi T, Solter D. Fatal flaws in the case for prepatterning in the mouse egg. Reprod Biomed Online 2006; 12:150–152.
4. Herr JC, Chertihin O, Digilio L, Jha KN, Vemuganti S, Flickinger CJ. Distribution of RNA binding protein MOEP19 in the oocyte cortex and early embryo indicates pre-patterning related to blastomere polarity and trophectoderm specification. Dev Biol 2008; 314:300–316.
5. Wolpert L, Tickle C, Lawrence P, Meyerowitz E, Robertson E, Smith J, Jessell T. Vertebrate development II: axes and germ layers. In: Wolpert L, Tickle C (eds.), Principles of Development, 4th ed. Oxford: Oxford University Press; 2011:93–127.
6. Fujimori T, Kurotaki Y, Komatsu K, Nabeshima Y. Morphological organization of the mouse preimplantation embryo. Reprod Sci 2009; 16: 171–177.
7. Feuer S, Rinaudo P. Preimplantation stress and development. Birth Defects Res C Embryo Today 2012; 96:299–314.
8. Gilbert SF. Birds and mammals: early development and axis formation. In: Developmental Biology, 9th ed. Sunderland, MA: Sinauer Associates; 2010:287–322.
9. Guo G, Huss M, Tong GQ, Wang C, Li Sun L, Clarke ND, Robson P. Resolution of cell fate decisions revealed by single-cell gene expression analysis from zygote to blastocyst. Dev Cell 2010; 18:675–685.
10. McDole K, Xiong Y, Iglesias PA, Zheng YX. Lineage mapping the preimplantation mouse embryo by two-photon microscopy, new insights into the segregation of cell fates. Dev Biol 2011; 355:239–249.
11. Niakan KK, Han J, Pedersen RA, Simon C, Pera RA. Human preimplantation embryo development. Development 2012; 139:829–841.
12. Xenopoulos P, Nowotschin S, Hadjantonakis A-K. Live imaging fluorescent proteins in early mouse embryos. In: Conn PM (ed.), Methods in Enzymology, vol. 506. Oxford: Academic Press 2012; 361–389.
13. Yamanaka Y, Ralston A. Early embryonic cell fate decisions in the mouse. In: Meshorer E, Plath K (eds.), The Cell Biology of Stem Cells. Boston, MA: Springer; 2010:1–13.
14. Bischoff M, Parfitt DE, Zernicka-Goetz M. Formation of the embryonic-abembryonic axis of the mouse blastocyst: relationships between orientation of early cleavage divisions and pattern of symmetric/asymmetric divisions. Development 2008; 135:953–962.
15. Fujimori T, Kurotaki Y, Miyazaki J, Nabeshima Y. Analysis of cell lineage in two- and four-cell mouse embryos. Development 2003; 130: 5113–5122.
16. Gardner RL. The axis of polarity of the mouse blastocyst is specified before blastulation and independently of the zona pellucida. Hum Reprod 2007; 22:798–806.
17. Katayama M, Roberts RM. The effect of superovulation on the contributions of individual blastomeres from 2-cell stage CF1 mouse embryos to the blastocyst. Int J Dev Biol 2010; 54:675–681.
18. Liu Z, Hai T, Dai X, Zhao X, Wang Y, Brochard V, Zhou S, Wan H, Zhang H, Wang L, Zhou Q, Beaujean N. Early patterning of cloned mouse embryos contributes to post-implantation development. Dev Biol 2012; 368:304–311.
19. Piotrowska K, Wianny F, Pedersen RA, Zernicka-Goetz M. Blastomeres arising from the first cleavage division have distinguishable fates in normal mouse development. Development 2001; 128:3739–3748.
20. Piotrowska K, Zernicka-Goetz M. Early patterning of the mouse embryo–contributions of sperm and egg. Development 2002; 129:5803–5813.
21. Piotrowska-Nitsche K, Perea-Gomez A, Haraguchi S, Zernicka-Goetz M. Four-cell stage mouse blastomeres have different developmental properties. Development 2005; 132:479–490.
22. Torres-Padilla ME, Parfitt DE, Kouzarides T, Zernicka-Goetz M. Histone arginine methylation regulates pluripotency in the early mouse embryo. Nature 2007; 445:214–218.
23. Kurotaki Y, Hatta K, Nakao K, Nabeshima Y, Fujimori T. Blastocyst axis is specified independently of early cell lineage but aligns with the ZP shape. Science 2007; 316:719–723.
24. Motosugi N, Bauer T, Polanski Z, Solter D, Hiiragi T. Polarity of the mouse embryo is established at blastocyst and is not prepatterned. Genes Dev 2005; 19:1081–1092.
25. Waksmundzka M, Wisniewska A, Maleszewski M. Allocation of cells in mouse blastocyst is not determined by the order of cleavage of the first two blastomeres. Biol Reprod 2006; 75:582–587.
26. Wennekamp S, Mesecke S, Nedelec F, Hiiragi T. A self-organization framework for symmetry breaking in the mammalian embryo. Nat Rev Mol Cell Biol 2013; 14:452–459.
27. Alarcon VB, Marikawa Y. Deviation of the blastocyst axis from the first cleavage plane does not affect the quality of mouse postimplantation development. Biol Reprod 2003; 69:1208–1212.
28. Alarcon VB, Marikawa Y. Spatial alignment of the mouse blastocyst axis across the first cleavage plane is caused by mechanical constraint rather than developmental bias among blastomeres. Mol Reprod Dev 2008; 75: 1143–1153.
29. Cockburn K, Rossant J. Making the blastocyst: lessons from the mouse. J Clin Invest 2010; 120:995–1003.
30. Johnson MH. From mouse egg to mouse embryo: polarities, axes, and tissues. Annu Rev Cell Dev Biol 2009; 25:483–512.
31. Maalouf WE, Alberio R, Campbell KH. Differential acetylation of histone H4 lysine during development of in vitro fertilized, cloned and parthenogenetically activated bovine embryos. Epigenetics 2008; 3: 199–209.
32. Moriyoshi K, Richards LJ, Akazawa C, O'Leary DD, Nakanishi S. Labeling neural cells using adenoviral gene transfer of membrane-targeted GFP. Neuron 1996; 16:255–260.
33. Alarcon VB, Marikawa Y. Unbiased contribution of the first two blastomeres to mouse blastocyst development. Mol Reprod Dev 2005; 72:354–361.
34. Bo GA, Mapletoft RJ. Evaluation and classification of bovine embryos. Anim Reprod 2013; 10:344–348.
35. Khan DR, Dube D, Gall L, Peynot N, Ruffini S, Laffont L, Le Bourhis D, Degrelle S, Jouneau A, Duranthon V. Expression of pluripotency master regulators during two key developmental transitions: EGA and early lineage specification in the bovine embryo. PLoS One 2012; 7:e34110.
36. Leidenfrost S, Boelhauve M, Reichenbach M, Gungor T, Reichenbach HD, Sinowatz F, Wolf E, Habermann FA. Cell arrest and cell death in mammalian preimplantation development: lessons from the bovine model. PLoS One 2011; 6:e22121.
37. Kim K, Park S, Roh S. Lipid-rich blastomeres in the two-cell stage of porcine parthenotes show bias toward contributing to the embryonic part. Anim Reprod Sci 2012; 130:91–98.

38. Park SK, Won C, Choi YJ, Kang H, Roh S. The leading blastomere of the 2-cell stage parthenogenetic porcine embryo contributes to the abembryonic part first. J Vet Med Sci 2009; 71:569–576.
39. Hosseini SM, Moulavi F, Tanhaie-Vash N, Asgari V, Ghanaei HR, Abedi-Dorche M, Jafarzadeh N, Gourabi H, Shahverdi AH, Dizaj AV, Shirazi A, Nasr-Esfahani MH. The principal forces of oocyte polarity are evolutionary conserved but may not affect the contribution of the first two blastomeres to the blastocyst development in mammals. PLoS One 2016; 11:e0148382.
40. Piotrowska-Nitsche K, Zernicka-Goetz M. Spatial arrangement of individual 4-cell stage blastomeres and the order in which they are generated correlate with blastocyst pattern in the mouse embryo. Mech Dev 2005; 122:487–500.
41. Topper EK, Kruijt L, Calvete J, Mann K, Topfer-Petersen E, Woelders H. Identification of bovine zona pellucida glycoproteins. Mol Reprod Dev 1997; 46:344–350.
42. Goolam M, Scialdone A, Graham SJ, Macaulay IC, Jedrusik A, Hupalowska A, Voet T, Marioni JC, Zernicka-Goetz M. Heterogeneity in Oct4 and Sox2 targets biases cell fate in 4-cell mouse embryos. Cell 2016; 165:61–74.
43. White MD, Angiolini JF, Alvarez YD, Kaur G, Zhao ZW, Mocskos E, Bruno L, Bissiere S, Levi V, Plachta N. Long-lived binding of Sox2 to DNA predicts cell fate in the four-cell mouse embryo. Cell 2016; 165: 75–87.
44. Holm P, Shukri NN, Vajta G, Booth P, Bendixen C, Callesen H. Developmental kinetics of the first cell cycles of bovine in vitro produced embryos in relation to their in vitro viability and sex. Theriogenology 1998; 50:1285–1299.
45. Chroscicka A, Komorowski S, Maleszewski M. Both blastomeres of the mouse 2-cell embryo contribute to the embryonic portion of the blastocyst. Mol Reprod Dev 2004; 68:308–312.
46. Kochhar HS, Kochhar KP, Basrur PK, King WA. Influence of the duration of gamete interaction on cleavage, growth rate and sex distribution of in vitro produced bovine embryos. Anim Reprod Sci 2003; 77:33–49.
47. Bermejo-Alvarez P, Rizos D, Rath D, Lonergan P, Gutierrez-Adan A. Epigenetic differences between male and female bovine blastocysts produced in vitro. Physiol Genomics 2008; 32:264–272.
48. Garcia-Herreros M, Aparicio IM, Rath D, Fair T, Lonergan P. Differential glycolytic and glycogenogenic transduction pathways in male and female bovine embryos produced in vitro. Reprod Fertil Dev 2012; 24:344–352.
49. Su J, Wang Y, Li W, Gao M, Ma Y, Hua S, Quan F, Zhang Y. Effects of 3-hydroxyflavone on the cellular and molecular characteristics of bovine embryos produced by somatic-cell nuclear transfer. Mol Reprod Dev 2014; 81:257–269.
50. Koo DB, Kang YK, Choi YH, Park JS, Kim HN, Oh KB, Son DS, Park H, Lee KK, Han YM. Aberrant allocations of inner cell mass and trophectoderm cells in bovine nuclear transfer blastocysts. Biol Reprod 2002; 67:487–492.
51. Jiang Z, Sun J, Dong H, Luo O, Zheng X, Obergfell C, Tang Y, Bi J, O'Neill R, Ruan Y, Chen J, Tian XC. Transcriptional profiles of bovine in vivo pre-implantation development. BMC Genomics 2014; 15:756.
52. Tominaga K, Hamada Y. Efficient production of sex-identified and cryosurvived bovine in-vitro produced blastocysts. Theriogenology 2004; 61:1181–1191.
53. Park JH, Lee JH, Choi KM, Joung SY, Kim JY, Chung GM, Jin DI, Im KS. Rapid sexing of preimplantation bovine embryo using consecutive and multiplex polymerase chain reaction (PCR) with biopsied single blastomere. Theriogenology 2001; 55:1843–1853.